Phase stability of highly compressed cesium

K. Takemura
National Institute for Research in Inorganic Materials, Namiki 1-1, Tsukuba, Ibaraki 305-0044, Japan

N. E. Christensen
Institute of Physics and Astronomy, Aarhus University, DK-8000 Aarhus C, Denmark

D. L. Novikov
Arthur D. Little Inc., Acorn Park, Cambridge, Massachusetts 02140-2390

K. Syassen*
Max-Planck-Institut für Festkörperforschung, Heisenbergstrasse 1, D-70569 Stuttgart, Germany

U. Schwarz
Max-Planck-Institut für Chemische Physik fester Stoffe, Pirnaer Landstrasse 176, D-01257 Dresden, Germany

M. Hanfland
European Synchrotron Radiation Facility, BP 220, F-38043 Grenoble, France
(Received 24 November 1999)

The crystal structure of cesium at pressures above ~70 GPa has been investigated using angle-dispersive powder x-ray-diffraction techniques. The modification Cs-VI is found to be double hexagonal close packed (dhcp), which is one of the two possible arrangements proposed earlier. No other phase transition is observed at pressures up to 184(20) GPa. We also present *ab initio* calculations of the pressure-dependent enthalpies of the phases Cs-IV (tetragonal), Cs-V (orthorhombic), and Cs-VI relative to that of a hcp lattice. In these calculations all structural parameters were optimized. The theoretical results are in full agreement with the experimentally observed phase transition sequence and structural parameters.

I. INTRODUCTION

Cesium undergoes a series of structural phase transitions under high pressure. Six modifications are known to exist at room temperature: I (bcc), II (fcc), III (collapsed fcc), IV (tetragonal), V (orthorhombic), and VI (hcp or double hexagonal close packed).[1–4] The pressure-driven electronic $s \rightarrow d$ transition in Cs (Ref. 5) is believed to play a major role in the structural behavior, at least for pressures up to about 15 GPa corresponding to fourfold compression.[6–9] Remarkable features of the phase transition sequence are the isostructural fcc-fcc transition[1] and the occurrence of the tetragonal phase IV (4.4–12 GPa) with an eightfold atom coordination.[2] The unusual decrease of the coordination number with increasing pressure from 12 in fcc to 8 in Cs-IV has been interpreted in terms of a different bonding induced by the s-d transition.[9,10] Beyond phase IV the coordination number again increases with pressure. The recently determined orthorhombic structure of Cs-V (12 to ~70 GPa, space group $Cmca$, $oC16$ in Pearson notation) has two nonequivalent crystallographic sites with coordination numbers of 10 and 11, respectively.[3]

In the present work we report an angle-dispersive x-ray-diffraction study of phase Cs-VI. The crystal structure of this phase, which was observed to appear near 72 GPa on increasing pressure, has been investigated earlier up to 92 GPa.[4] At these pressures, where Cs is compressed to about 20% of its ambient pressure volume, a close-packed structure is predicted to be favored by the strong core repulsion.[9] The earlier x-ray-diffraction patterns of phase VI could be indexed either with the hcp or the double hexagonal-close-packed (dhcp) structure. The crystal structure assignment remained ambiguous partly because of phase coexistence. Our experimental results clearly show the structure of Cs-VI to be dhcp, with an axial ratio similar to that for ideal close packing of spheres.

We have furthermore theoretically explored the phase stability of Cs using density-functional theory. Four different crystal structures were considered, the tetragonal Cs-IV type, the orthorhombic Cs-V type, hcp and dhcp. According to earlier total-energy calculations,[9] which were based on the linear muffin tin orbital (LMTO) method,[11] the $5p$ core states of Cs are significantly broadened at pressures above 10 GPa. The stable structures under such conditions were predicted to be hcp at $P > 15$ GPa, followed by bcc at $P > 220$ GPa. In the calculations presented here we have used a full-potential version of the LMTO method.[12,13] In contrast to the earlier calculations the hcp structure is found to be the highest in enthalpy throughout the pressure range from 5 to 200 GPa. Our theoretical results predict a phase transition sequence in very good agreement with the experimental results.

II. X-RAY-DIFFRACTION STUDIES

Cs metal with a stated purity of 99.95% was enclosed in a Re gasket under silicone oil and pressurized in a diamond

anvil cell (DAC) using bevelled diamond anvils. The initial diameter of the gasket hole varied between 40 and 60 μm. Pressures up to 100 GPa were measured by the ruby luminescence method.[14] At pressures above 100 GPa the ruby luminescence signal became too weak, and therefore pressures were estimated from the *d* spacings of reflections from the Re gasket[15,16] measured with the x-ray beam positioned at the inner rim of the gasket hole. As a crosscheck, a Pt marker[17] was used in one experimental run carried out at pressures from 91 to 116 GPa. Angle-dispersive powder x-ray diffraction experiments have been carried out at the Photon Factory (PF) and the European Synchrotron Radiation Facility (ESRF). Experiments at the PF were performed on the bending magnet beam line 18C using a monochromatic beam with an energy of 20.00 keV.[18] Those at the ESRF were carried out at the undulator beam line ID9 using 27.42 keV radiation. Diffraction patterns were recorded on image plates. In the ESRF experiments the DAC was rocked by $\pm 0.5°$ to achieve better powder averaging. The image plate was placed at a large distance (0.45 m) from the sample in order to improve the angular resolution. Typical exposure times were 30 min at the PF and 3 min at the ESRF. Diffraction images were analyzed using standard pattern integration software.[19] All diffraction experiments were performed at room temperature.

Figure 1 shows selected powder diffraction patterns of Cs at different pressures between 56 and 90 GPa, covering the transition regime from Cs-V to Cs-VI. Up to about 65 GPa, diffraction patterns characteristic of the $oC16$ ($Cmca$) phase are observed (cf. the observed and calculated diagram at 56 GPa shown in Fig. 1). At room temperature the transition to Cs-VI is sluggish. It starts at about 68 GPa, as indicated by intensity changes and the appearance of new diffraction peaks in the powder diagrams. The transition is completed at around 95 GPa. Above 95 GPa the diffraction patterns show very little change with pressure.

In order to obtain well-resolved diffraction patterns of single-phase Cs-VI, a Cs sample at 90 GPa was annealed at 140° C for 3.5 h and subsequently at 180° C for 6.5 h. The pattern at 88 ± 4 GPa shown in Fig. 1 corresponds to that of the annealed sample. For comparison, calculated patterns for the dhcp structure and for the corresponding hcp arrangement are also shown in Fig. 1. The observation of the reflections 101, 103, and 105 in the experimental pattern clearly indicates that Cs-VI has a dhcp structure rather than a hcp structure. Small discrepancies between calculated and experimental integrated diffraction intensities are attributed to preferred orientation effects.

On the basis of our diffraction data taken in the transition regime from Cs-V to Cs-VI, we cannot fully rule out that the dhcp phase of Cs-VI comes with some admixture of hcp structure. A quantitative estimate of phase ratios is difficult due to correlations between preferred orientation effects and phase mixture. However, the fact that at pressures above 90 GPa all reflections characteristic for dhcp structure are seen with approximately the expected relative intensities clearly shows that the dhcp phase is the dominant phase. Diffraction patterns consistent with a dhcp structure were observed up to the highest pressure (~ 184 GPa, $V/V_0 = 0.1385$) reached in our experiments.

The pressure-volume (PV) data of Cs-VI are plotted in

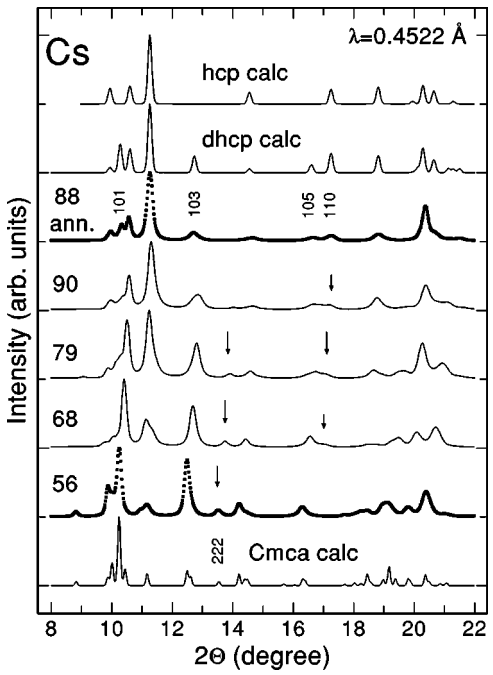

FIG. 1. Powder x-ray-diffraction patterns of Cs taken at the ESRF. The diagrams are for phases Cs-V (56 GPa) and Cs-VI (88 GPa, annealed) and for mixed phases (68, 79 and 90 GPa). The arrows point to nonoverlapping diffraction peaks of Cs-V (222) and Cs-VI (110), which decrease and increase, respectively, in intensity with increasing pressure. For comparison, calculated diffraction patterns are shown for the $oC16$ ($Cmca$) phase of Cs-V [$a = 9.937$ Å and $b = c = 5.880$ Å], the dhcp structure of Cs-VI [$a = 3.015(4)$ Å and $c = 9.790(15)$ Å], and a corresponding hcp arrangement.

Fig. 2, which also shows experimental PV data for Cs-V from this work and the low-pressure data points for Cs-V given in Ref. 3. The experimental volume difference between Cs-V and Cs-VI amounts to $2.0 \pm 1\%$. In Fig. 2 the solid lines drawn through the experimental data correspond to fitted Vinet relations[20]

$$P - P_0 = 3B_0\rho^{-2}(1-\rho)\exp(\eta),$$

$$\rho = (V/V_0)^{1/3},$$

$$\eta = 1.5(B' - 1)(1-\rho). \tag{1}$$

Here P_0 and V_0 are the reference pressure and volume, respectively, and B_0 and B' refer to the bulk modulus and its pressure derivative, respectively, at (P_0, V_0). The corresponding parameter values are given in Table I. Because of the large uncertainty in the pressure determination at pressures above 100 GPa, the parameter B' of Cs-VI was fixed at a value of 4.

Figure 3 shows the experimental axial ratios a/c and $c/2a$ of Cs-V and Cs-VI, respectively, as a function of volume. The extremely small deviation of the orthorhombic structure of Cs-V from a tetragonal metric ($b/c = 1.005$ at 12 GPa; see Ref. 3) is not resolved at pressures above 30 GPa. In the region of coexistence of both phases the experimental axial ratios suffer from large errors due to strong overlap between Cs-V and Cs-VI reflections. Above 100 GPa (V_{atom}

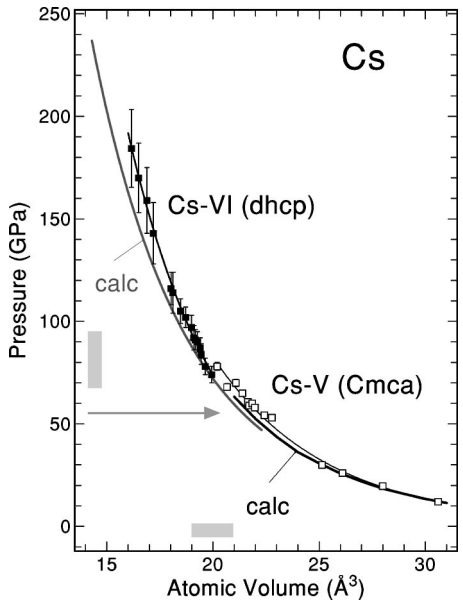

FIG. 2. Pressure-volume relation for Cs. Open and closed symbols represent experimental data for Cs-V ($oC16$,$Cmca$) and Cs-VI (dhcp), respectively, at 300 K. The error bars indicate the estimated experimental uncertainties (see the text). The thin lines passing through the experimental data points refer to fitted Vinet relations [Eq. (1)]. The gray bars indicate the region of coexistence of phases V and VI in the experiments. At the highest experimental pressure [184(20) GPa], Cs is compressed to 13.85(5)% of its ambient pressure volume. The solid lines marked calc represent our calculated PV relations for Cs (static lattice limit) in the $oC16$ ($Cmca$) and dhcp phases. The horizontal arrow indicates the calculated phase transition pressure.

<18.5 Å^3) the $c/2a$ ratio of dhcp Cs adopts a value close to that for an ideal close-packed dhcp structure ($c/2a=1.63$).

III. THEORETICAL RESULTS

We have theoretically examined the stability of four crystal structures (tetragonal Cs-IV, orthorhombic Cs-V, hcp, and dhcp) using the local approximation to the density-functional theory (LDA) as well as generalized gradient approximations (GGA). The results presented here were obtained by application of the Perdew-Burke-Ernzerhof scheme.[21] We did, however, choose the parameter κ, which

TABLE I. Fitted equation-of-state parameters [Vinet relation, Eq. (1)] for the phases Cs-V and Cs-VI. V_0, B_0, and B' are the atomic volume, bulk modulus, and pressure derivative of the bulk modulus at the reference pressure P_0. Errors refer to 95% confidence limits. The last row lists corresponding parameters for the calculated PV relation of rhenium (see the Appendix).

	P_0 (GPa)	V_0 (Å^3)	B_0 (GPa)	B'
Cs-V (expt.)	12	30.60	65(12)	4.7(10)
Cs-V (theor.)	11.4	31.12	51	5.06
Cs-VI (expt.)	74	19.92(10)	330(40)	4 (fixed)
Cs-VI (theor.)	72.1	19.99	279.6	3.49
Re (theor.)	−3.9	14.686	371	4.19

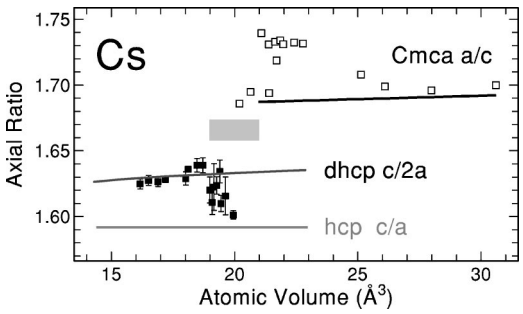

FIG. 3. Axial ratios a/c, $c/2a$, and c/a for the $oC16$ ($Cmca$), dhcp, and hcp phases, respectively, of Cs as a function of atomic volume. The symbols represent experimental data, and the solid lines refer to the calculated results.

is associated with the degree of localization of the exchange-correlation hole, to be 0.45 (in accordance with our previous estimations,[22]) i.e., smaller than the ''standard value'' of 0.806 (Ref. 21). The LDA calculations lead to a non-negligible overbinding in Cs. For example, the theoretical equilibrium volume of bcc Cs calculated from the electronic LDA total energies alone is $\sim 12\%$ smaller than the experimental value at room temperature. Applying the GGA we find[23] that the electronic isotherm of bcc Cs has zero pressure for a volume, which is 4% smaller than the observed one. If, in addition, the contributions from phonons to the energy and entropy are taken properly into account, we find[23] that the GGA yields an equilibrium volume at $T=290$ K which is only 2% too large, i.e., it is in good agreement with experiment. The calculations presented here do not include thermal effects. We only need structural energy *differences*, and the corrections of these differences due to the phonons are expected to be small. Also, full phonon calculations for the rather complex structures in the relevant pressure range are rather demanding in our scheme.

Structural parameters were optimized by minimizing the total energy through the application of what essentially is a steepest-descent method. Atomic coordinates as well as cell dimensions are optimized simultaneously at a constant volume value. The solution of the effective one-electron equations was performed by means of the LMTO method[11] in the full-potential version.[12,13] The semi core states, Cs-5s and -5p, are treated as *local orbitals*[24,25] in the same energy window as the valence states.

The calculated PV relations of Cs-V and Cs-VI and the axial ratios as a function of volume are shown in Figs. 2 and 3, respectively. Numerical fits of the Vinet relation [Eq. (1)] to the calculated PV relations yield the parameter values listed in Table I. For Cs-V and Cs-VI the results are close to the experimental values. We note however, that at small volumes the estimated experimental pressures are significantly higher than the calculated pressures. There is no indication that the experimental equation of state of rhenium, which was used for pressure calibration in this range, may be in error. On the contrary, our calculated PV relation of Re (see the Appendix) agrees extremely well with the available experimental data. Therefore, the discrepancy between our calculated results and the experimental PV data of Cs above 100 GPa may arise from rather large uncertainties in the pressure values derived from the rhenium gasket reflections. The likely reasons for this are pressure gradients across the

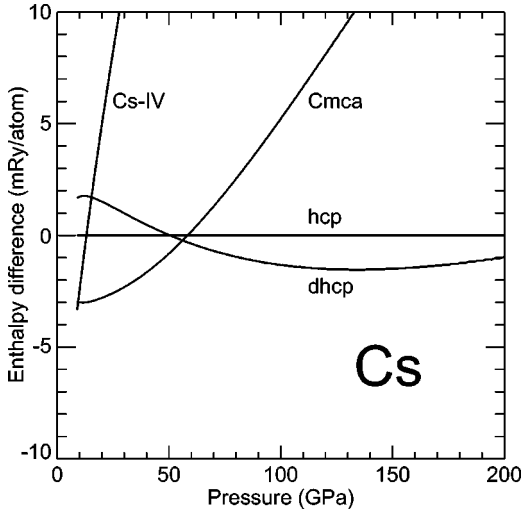

FIG. 4. Calculated enthalpy differences (relative to hcp) for different phases of Cs as a function of calculated pressure. The enthalpy values refer to optimized structural parameters. The calculated phase transition pressures are 10(3) GPa for Cs-IV (tetragonal) to Cs-V (orthorhombic) and 55(5) GPa for Cs-V to Cs-VI (dhcp).

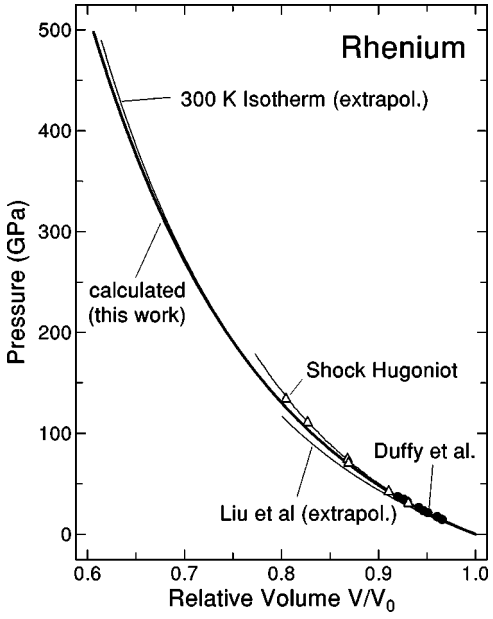

FIG. 5. Pressure-volume relation of rhenium. V_0 refers to the experimental equilibrium volume at 300 K. The solid line is the calculated zero-temperature (static lattice) isotherm. The open triangles refer to shock Hugoniot data (Ref. 16), the curve marked Liu *et al.* is an extrapolation of the experimental results from Ref. 34, and the full dots represent data from recent x-ray-diffraction measurements (Ref. 35). The line marked ''300 K Isotherm'' corresponds to the Birch relation of Ref. 15.

center part of the diamond tip as well as deviatoric stresses, for which we have not applied any corrections. For the data taken at the highest pressures we estimate the corresponding uncertainties in sample pressure determination to be about 10%, as indicated by the error bars shown in Fig. 2.

For both phases of Cs the respective calculated axial ratios are nearly constant, with a weak tendency to decrease with increasing compression for Cs-V. Taking into account the experimental uncertainties, the calculated axial ratios agree with the experimental data. The theoretical values for $c/2a$ in the dhcp structure of Cs are close to 1.632, which clearly differs from $c/a \approx 1.592$ calculated for the hcp phase. This might serve, when compared to experimental results, as an additional evidence of the dhcp phase existence rather than hcp. The theoretical a/c value for Cs-V which is indicated in Fig. 3 corresponds to 1.691. The other structural parameters obtained from the optimization of the $oC16$ ($Cmca$) phase are axial ratio $b/c=1.011$, positional parameter $x=0.2148$ for the Wyckoff position $8d(x,0,0)$, and $y=0.1759$ and $z=0.3256$ for $8f(0,y,z)$. The corresponding experimental values[3] at 12 GPa are $a/c=1.699$, $b/c=1.005$, $x=0.216$, $y=0.173$, and $z=0.327$. We note that our calculations for Cs-V reproduce even subtle structural effects like for instance, the very small deviation from tetragonal symmetry.

Figure 4 shows the calculated enthalpies vs pressure for the four modifications of Cs considered here. Allowing for ± 0.5-m Ry numerical error in the total energies, the calculations suggest that the Cs-V structure has the lowest enthalpy between 10 ± 3 and 55 ± 5 GPa. The dhcp structure is lowest in enthalpy above 55 GPa all the way up to at least 200 GPa. Thus the calculated equilibrium transition pressures for zero temperature (static lattice) agree very well with the ambient temperature experimental data on the Cs-IV to Cs-V transition, and on the Cs-V to Cs-VI transition.

The present calculation suggests that the dhcp structure is stable relative to the hcp structure over a wide range of pressures (55 GPa to at least 200 GPa). This differs from the earlier calculation[9] using the LMTO method in the atomic spheres approximation (ASA).[11] These earlier theoretical results indicate that among the structures considered (fcc, bcc, dhcp, Sm-type, and hcp) the hcp structure is most stable above 15 GPa, followed by the bcc structure above 220 GPa. The dhcp structure had always higher total energy than the hcp structure. Although the ASA has been useful in predicting trends[26] in structural properties, its accuracy may not be sufficient to predict details for a specific material.

IV. REMARKS AND CONCLUSIONS

The phase transition sequence from Cs-IV via Cs-V to Cs-VI is similar to the transition sequence in Si under high pressure.[27,28] The hexagonal primitive phase Si-V (16–38 GPa) is closely related to the tetragonal phase Cs-IV. The main difference is in the arrangement of trigonal prisms; in the hexagonal primitive structure the prisms are all oriented in parallel, whereas in the Cs-IV structure the orientation alternates by 90° in subsequent layers along the c axis.[29] The high-pressure phase Si-VI (38–45 GPa) is isostructural and even isotypic to Cs-V.[27] Si-VI transforms to the hcp structure ($c/a=1.693$) at higher pressures, whereas in the case of Cs the transformation is to dhcp structure instead. Si exhibits an extended coexistence range (42 to ~49 GPa) of the $oC16$ and hcp structures.[27] The mixed-phase region of Cs-V and VI is also large, spanning from ~68 to ~95 GPa. This indicates small enthalpy differences in both cases, which is supported by the results of the theoretical calculations presented here and in Ref. 28. The preference for dhcp structure in Cs as compared to hcp structure in Si cannot be explained

by a simple argument, because after all the energy differences between these two structures are very small, of the order of 1 m Ry/atom.

The dhcp structure is observed for several rare-earth metals at atmospheric or high pressure.[30,31] The well-known structural sequence of rare earth metals under high pressure (hcp–Sm-type–dhcp–fcc) has been correlated with the *d*-band occupancy.[32] The dhcp phase of Cs does not readily fit into this scheme, because the $s \rightarrow d$ transition is already completed near 15 GPa, and core-core repulsion as well as *p*-*d* hybridization are quite important in Cs at the volume where the dhcp phase comes into play. Although it is not possible in our theoretical method to estimate exactly the $s \rightarrow d$ charge transfer induced by the volume decrease (the electrons in the interstitial sites cannot be assigned to a particular atomic orbital), we consistently observe higher electron population of the valence 6*s* states and lower population of 5*d* states inside the atomic spheres for the hcp structure as compared to corresponding calculations for the dhcp structure at the same volume per atom.

In summary, we have investigated the structural behavior of highly compressed cesium. The structure of Cs-VI is found to be dhcp, with a $c/2a$ ratio corresponding to that of an ideal close packing of spheres. The phase Cs-VI is observed to be stable up to at least 184(20) GPa. The results of our first-principles calculations for several high-pressure phases of Cs are found to be in very good agreement with the experimental structural parameters as well as phase transition pressures. With the present results, structural information is available for all high pressure phases of Cs up to about 184 GPa. The only exception is the phase Cs-III, for which the collapsed fcc structure was not confirmed in recent diffraction studies.[3,33] Neither do finite-*T* calculations[23] support the possibility of an fcc→fcc (i.e., isostructural) transition in Cs.

ACKNOWLEDGMENTS

We thank I. Loa, A. Grzechnik, T. Ino, and H. Nakao for their help in the measurements. The experiments at the Photon Factory were performed under Proposal Nos. 93G105 and 95G138.

APPENDIX

The isothermal PV relation of rhenium[15] used in this work for pressure calibration above 100 GPa is based on shock wave data.[16] In order to check whether this isotherm is consistent with predictions from first-principles theory, we have calculated the PV relation of hcp rhenium in the pressure range up to 500 GPa using LDA theory and the full-potential LMTO method. Optimizations of the c/a ratio give values between 1.62 and 1.61 for $0 < P < 500$ GPa. The calculated PV relation is shown in Fig. 5. The zero-pressure atomic volume is obtained as 14.55 Å^3, i.e., it agrees to within 1% with the experimental volume ($V_0 = 14.686$ Å^3/atom at 300 K). For the bulk modulus and its pressure derivative at the experimental V_0 (calculated pressure $P_0 = -3.09$ GPa) we obtain $B_0 = 371$ GPa and $B' = 4.19$. For comparison, Vohra *et al.*[15] gave $B_0 = 372$ GPa and $B' = 4.05$ for these parameter values, obtained from a Birch-Murnaghan fit to the 300-K isotherm. We note a very good overall agreement of our theoretical results and the available experimental PV data for rhenium. Furthermore, the validity of the isothermal PV relation of Re (Ref. 15) up to pressures of 500 GPa is supported by the results of our calculations. Inserting our calculated equation of state parameters into Eq. (1) results in a PV curve which, at the highest pressure of 500 GPa, deviates by less than 0.5 GPa from our calculated pressure (see Fig. 5).

*Author to whom correspondence should be addressed. Electronic address: syassen@servix.mpi-stuttgart.mpg.de

[1] H.T. Hall, L. Merrill, and J.D. Barnett, Science **146**, 1297 (1964).

[2] K. Takemura, S. Minomura, and O. Shimomura, Phys. Rev. Lett. **49**, 1772 (1982).

[3] U. Schwarz, K. Takemura, M. Hanfland, and K. Syassen, Phys. Rev. Lett. **81**, 2711 (1998).

[4] K. Takemura, O. Shimomura, and H. Fujihisa, Phys. Rev. Lett. **66**, 2014 (1991).

[5] R. Sternheimer, Phys. Rev. **78**, 235 (1950).

[6] S.G. Louie and M.L. Cohen, Phys. Rev. B **10**, 3237 (1974).

[7] A.K. McMahan, Phys. Rev. B **17**, 1521 (1978).

[8] D. Glötzel and A.K. McMahan, Phys. Rev. B **20**, 3210 (1979).

[9] A.K. McMahan, Phys. Rev. B **29**, 5982 (1984).

[10] N.E. Christensen, Z. Pawlowska, and O.K. Andersen (unpublished).

[11] O.K. Andersen, Phys. Rev. B **12**, 3060 (1975).

[12] M. Methfessel, Phys. Rev. B **38**, 1537 (1988).

[13] M. Methfessel and M. van Schilfgaarde (unpublished and private communication).

[14] H.K. Mao, P.M. Bell, J.W. Shaner, and D.J. Steinberg, J. Appl. Phys. **49**, 3276 (1978).

[15] Y.K. Vohra, S.J. Duclos, and A.L. Ruoff, Phys. Rev. B **36**, 9790 (1987). The isothermal equation of state for Re given in this reference is based on the reduced shock wave data of Ref. 16.

[16] R.G. McQueen, S.P. Marsh, J.W. Taylor, J.N. Fritz, and W.J. Carter, in *High Velocity Impact Phenomena*, edited by R. Kinslow (Academic, New York, 1970), p. 293.

[17] N.C. Holmes, J.A. Moriarty, G.R. Gathers, and W.J. Nellis, J. Appl. Phys. **66**, 2962 (1989).

[18] O. Shimomura, K. Takemura, H. Fujihisa, Y. Fujii, Y. Ohishi, T. Kikegawa, Y. Amemiya, and T. Matsushita, Rev. Sci. Instrum. **63**, 967 (1992).

[19] A.P. Hammersley, S.O. Svensson, M. Hanfland, A.N. Fitch, and D. Häusermann, High Press. Res. **14**, 235 (1996); H. Fujihisa (unpublished).

[20] P. Vinet, J. Ferrante, J.R. Smith, and J.H. Rose, J. Phys. C **19**, L467 (1986).

[21] J.P. Perdew, K. Burke, and M. Ernzerhof, Phys. Rev. Lett. **77**, 3865 (1996).

[22] E. L. Peltzer y Blancá, C. O. Rodriguez, J. Shitu, D.L. Novikov (unpublished).

[23] N.E. Christensen, D. J. Boers, J. van Velsen, and D.L. Novikov, Phys. Rev. B **61**, R3764 (2000); J. Phys.: Condens. Matter **12**, 3293 (2000).

[24] D.J. Singh, *Planewaves, Pseudopotentials and the LAPW Method* (Kluwer, Boston 1994).

[25] M. van Schilfgaarde (unpublished).

[26] H.L. Skriver, Phys. Rev. B **31**, 1909 (1985).

[27] M. Hanfland, U. Schwarz, K. Syassen, and K. Takemura, Phys. Rev. Lett. **82**, 1197 (1999).

[28] N.E. Christensen, D.L. Novikov, and M. Methfessel, Solid State Commun. **110**, 615 (1999).
[29] M. O'Keeffe and B.G. Hyde, *Crystal Structures* (Mineralogical Society of America, Washington, DC, 1996), Vol. 1, p. 234.
[30] W.B. Holzapfel, J. Alloys Compd. **223**, 170 (1995).
[31] D.A. Young, *Phase Diagrams of the Elements* (University of California Press, Berkeley, 1991).
[32] J.C. Duthie and D.G. Pettifor, Phys. Rev. Lett. **38**, 564 (1977).
[33] A. Grzechnik, K. Syassen, U. Schwarz, and M. Hanfland (unpublished).
[34] L.G. Liu, T. Takahashi, and W.A. Bassett, J. Phys. Chem. Solids **31**, 1345 (1970).
[35] T.S. Duffy, G. Shen, D.L. Heinz, J. Shu, Y. Ma, H.K. Mao, R.J. Hemley, and A.K. Singh, Phys. Rev. B **60**, 15 063 (1999).